Journal of Thermal Analysis and Calorimetry, Vol. 90 (2007) 2, 431–441

THERMAL ANALYSIS OF BINARY LIQUID CRYSTALLINE MIXTURES
System of bent core and calamitic molecules

A. Bubnov[1*], *Věra Hamplová*[1], *M. Kašpar*[1], *Anikó Vajda*[2], *Maja Stojanović*[3], *Dusanka Ž. Obadović*[3], *N. Éber*[2] *and Katalin Fodor-Csorba*[2]

[1]Institute of Physics, Academy of Sciences of the Czech Republic, Na Slovance 2, 18221 Prague, Czech Republic
[2]Research Institute for Solid State Physics and Optics, Hungarian Academy of Sciences, 1525 Budapest, P.O. Box 49, Hungary
[3]Department of Physics, Faculty of Sciences, University of Novi Sad, Trg D. Obradovića 4, Novi Sad, Serbia and Montenegro

Two series of binary mixtures composed of bent shaped and rod like molecules are reported. The first star shaped bent core molecules were synthesized and used as a component of binary mixtures. The chiral rod like compounds having commensurable length with the arms of the bent core compounds have been chosen for these mixtures. The resulted compositions show various thermotropic liquid crystalline phases that are characteristic to both types of liquid crystalline materials. In case of mixing the rod like molecules to the bent core compound the B2, B7 and induced B1 phases have been observed. While using the star-shaped bent core and chiral rod like compounds in mixture, the paraelectric smectic A, ferroelectric smectic C* and orthogonal hexatic smectic B phases were preferred. The appearing mesophases were investigated by differential scanning calorimetry, polarizing optical microscopy and X-ray diffraction methods.

Keywords: *bent core molecules, binary mixtures, DSC, phase diagram, phase transition, rod like molecules, star-shaped bent core molecules*

Introduction

Bent shaped (or banana shaped) mesogens [1, 2] represent a new class of non-conventional thermotropic liquid crystals showing even more reach mesomorphic properties than the classical liquid crystals formed by rod like or disk like molecules. One of the most attractive aspects of the bent shaped materials is the unusual interplay between the chirality of the phases and of their forming layers, despite being formed from achiral molecules. At least seven phases, denoted B1-B7 have been disclosed in the bent core compounds, none of them being found in pure calamitic systems. According to the present knowledge, B3 belongs to crystal phase. Liquid crystalline phases, namely B2 [3, 4], B4 [5], B5 [6], and B7 [7] present properties deeply related to chirality. In the B2 phase, the molecules are tilted with respect to the layer normal and the layer chirality occurs due to the molecular tilting and molecular bent shape [8]: the molecules become switchable by applying an electric field. The structure of B4 phase is not fully understood yet, but the experimental observations reveal that it is composed of two segregated chiral domains with opposite optical rotatory power [9]. The layer spacing coincides with the molecular length [2, 10] attesting that the average molecular long axis is along the layer normal. Hence, the chiral origin of the B4 phase is different than that of the B2 phase and related to the twisted conformations of the molecules [11].

For the last decade, thermal and miscibility properties of the liquid crystalline materials with various molecule shapes have been studied intensively by various authors. In order to respond the application demands, the required liquid crystalline properties can be reached rather by mixing compounds with various molecular shapes and properties than by looking for the pure compounds with definite properties. Moreover, to the best of our knowledge, strong difficulties appear with obtaining a good alignment of the bent shaped compounds. Due to above mentioned reasons, many efforts have been done in order to establish the rules of molecular interactions using various liquid crystalline systems as liquid crystalline mixtures often yielded new phases and phase sequences not presented in either of the components. Doping of the ferroelectric SmC* phase with bent shaped molecules in some cases induces the antiferroelectric SmC$^*_A$ phase [12, 13]. Recently, D'have *et al.* [14] showed that the orthoconic antiferroelectric materials gives rise to the observation of the totally black ground state in surface stabilized planar oriented geometries that is of high potential use for fast electro-optic light modulators. Mixtures with various composition of calamitic molecules possessing the

---

[*] Author for correspondence: bubnov@fzu.cz

1388–6150/$20.00

Akadémiai Kiadó, Budapest, Hungary
Springer, Dordrecht, The Netherlands

ferroelectric SmC* phase with high tilt angle (θ≈45°) and bent core compounds possess the antiferroelectric phase with very high tilt angle even at relatively low concentrations (about 5 mol%) of the bent shaped compounds [15].

Very promising non-linear optic applications can be reached using large uniformly chiral domains of B4 phase that was confirmed while mixing bent shaped P-8-O-PIMB and rod (5CB) achiral molecules [11].

Occurrence the transitions between the B2 phase and typical mesophases of calamitic compounds in pure bent core mesogens (for example B2-SmA [16–18], B2-SmA-SmC [17, 18], B2-SmC-SmA-N [17–19]) stimulated the active studies of binary mixtures composed of the rod like and bent shaped molecules. The transitions between the ‘banana’ B2 phase and more usual smectic phases (in the sequences B2-SmA, B2-SmC, B2-SmC-SmA-N) had been found and studied [20]. Mixing of the bent shaped and rod like compounds can be useful also for clarifying the thermal and/or mesomorphic properties of one of the single compound [21].

The binary system reported by Prathiba *et al.* [22], shows a new type of orientational transition when the bent core molecules mixed in an anisotropic matrix made up of rod like molecules. At concentration of the bent core molecules below 13 mol%, a structural change takes place in which the symmetry axes point along the layer normal of the SmA_2 structure formed by rod like molecules [23]. For concentrations within 4–13 mol% of the bent core molecules, those molecules order themselves in the smectic layers with the director being orthogonal to the rod like molecules displaying the biaxial smectic A_2 (SmA_{2b}) phase [22]. Further studies on different system confirmed that the arrow axes of the bent core molecules are along the layer normal of the partial bilayer smectic structure formed by the rods [24, 25].

The aim of this work is to contribute to the understanding of miscibility effect on mesomorphic properties while mixing the banana shaped and rod like molecules possessing liquid crystalline behaviour. In particular two systems of mixtures had been selected and studied. The first system consists of the bent shaped compound *bis*[4-[(4’-*n*-decyloxy)biphenyloxycarbonyl]-4’-[2-methoxyphenyl]benzene-1,3-dicarboxylate (denoted as AI) [4], and chiral rod like compound (S)-2-pentyl-2-{[4-[4’’’-*n*-octyloxybenzoyloxy]-4’’-benzoyloxy]-4’-benzoyloxy]-propionate (denoted as AII) [26]. The second one is composed of the first star like banana-shaped bis {4-[4’-*n*-decyloxy-biphenyloxycarbonyl]-4’-[2-methoxy-phenyl]}-5-decyloxy-benzene-1,3-dicarboxylate (denoted as BI) and one chiral rod like compound (S)-4-{[4’-*n*-dodecyloxy-3’-methoxy-benzoyloxy]-biphenyloxy}-2-hexyloxy-propionate (denoted as BII) [27, 28].

Experimental

Materials

The chemical purity of the individual compounds was determined by high-performance liquid chromatography using an Ecom HPLC chromatograph and a silica gel column (Separon 7 μm, 3×350, Tessek) eluted with a mixture of toluene (99.9%) and methanol (0.1%). The elution profile was checked by a UV-Vis detector working at λ=290 nm. The chemical purity was better than 99.6%.

Structures of the intermediates and final products were checked by ^{1}H NMR (nuclear magnetic resonance) spectroscopy with a 200 MHz Varian spectrometer using tetramethylsilane as internal standard.

Synthesis

5-(*n*-alkyloxy)isophthalic acid (**1**) was synthesized by alkylation of diethyl ester of 5-hydroxyisophthalic acid (100 mmol) with decyl bromide (100 mmol) in dry ethanol/sodium ethanolate from 3 g of sodium metal. After the reaction was completed, the ester was hydrolysed by KOH (250 mmol) and 5-(*n*-alkyloxy)isophthalic acid was separated by acidification and further filtration (70 mmol, 70%).

The 5-*n*-(alkoxy)isophthalic acid dichloride (**2**), obtained by reaction of **1** (10 mmol) with thionyl chloride (100 mL). After 4 h reflux, the excess of thionyl chloride was removed and the residue was used without further purifications.

General procedure for preparation of *bis*[4’(*n*-decyloxy)biphenyloxycarbonyl]-4’[(3-methoxy) phenyl]-(2-methoxy)phenyl-5-*n*-alkoxy isophthalate BI: *n*=10, CI: *n*=4.

Compound **2** (10 mmol) in dry dichloromethane solution was added to a solution of 4-[(*n*-decyloxy)biphenyloxy)]-[(3-methoxy)-4-hydroxy]benzoate (**3**) (20 mmol) in dichloromethane/pyridine solution (100 mL/5 mL) and stirred under reflux for 2 days. The mixture was then poured into water and extracted with chloroform, washed with diluted HCl and evaporated. Row product was purified by column chromatography on silica gel (Kieselgel 60, (0.063–0.2 mm) using a mixture of dichloromethane (99.5%) and acetone (0.5%) as eluent. The appropriate fractions were collected, evaporated and the product was crystallized twice from acetone (2 g).

Bis{[4’-(*n*-decyloxy)biphenyloxycarbonyl]-4’[(2-methoxy) phenyl]}-5-(*n*-decyloxy-phenyl)

1,3-dicarboxylate (BI). ^{1}H-NMR ($CDCl_3$, 200 MHz) for compound: 8.62s (1H, HAr para to $C_{10}O$–); 8.00s (2H, HAr ortho to $C_{10}O$–); 7.95d (2H, HAr para to OCH_3–); 7.85s (2H, HAr ortho to OCH_3–); 7.50–7.60dd (8H, HAr ortho to Ar–Ar); 7.30m (6H, HAr ortho to –OCO); 7.00d (4H, HAr ortho to RO-Ar-biphenyl); 4.15t (2H, CH_2OAr in isophthalic acid); 4.00t (4H, CH_2OAr-biphenyl); 3.95s (6H, CH_3OAr); 1.80m (6H, CH_2CH_2OAr), 1.20–1.60m (42H, CH_2); 0.90t (9H, CH_3).

Bis[4'(*n*-butyloxy)biphenyloxycarbonyl]-4'[(3-methoxy)phenyl]-(2-methoxy)phenyl-5-(*n*-decyloxy)isophthalate (CI). ^{1}H-NMR ($CDCl_3$, 200 MHz) for compound CI: 8.62s (1H, HAr para to $C_{10}O$–); 8.00s (2H, HAr ortho to $C_{10}O$–); 7.95d (2H, HAr para to OCH_3–); 7.85s (2H, HAr ortho to OCH_3–); 7.50–7.60dd (8H, HAr ortho to Ar–Ar); 7.30m (6H, HAr ortho to –OCO); 7.00d (4H, HAr ortho to RO-Ar-biphenyl); 4.15t (2H, CH_2OAr in isophthalic acid); 4.00t (4H, CH_2OAr-biphenyl); 3.95s (6H, CH_3OAr); 1.80m (6H, CH_2CH_2OAr), 1.25–1.60m (30H, CH_2); 0.90t (9H, CH_3).

Methods

Sequence of phases and phase transition temperatures were determined on heating/cooling to/from the isotropic phase from characteristic textures and their changes observed in the polarising microscope (Nicon Eclipse E600POL). The Linkam LTS E350 heating stage with TMS 93 temperature programmer was used for the temperature control, which enabled temperature stabiliyation within ±0.1 K. Photos of the characteristic textures were obtained using Nicon Coolpix 990 digital camera, attached to the polarisying microscope. The width of all presented photos is about 400 μm.

Phase transition temperatures and transition enthalpies were evaluated from differential scanning calorimetry (DSC-Pyris Diamond, Perkin-Elmer 7) on cooling and heating runs at a rate of 5 K min^{-1}. The samples (1–5 mg) hermetically sealed in aluminium pans were placed in a nitrogen atmosphere. The temperature was calibrated on extrapolated onsets of melting points of water, indium and zinc. The enthalpy change was calibrated on enthalpies of melting of water, indium and zinc.

The electro-optic measurements were performed on 25 μm thick planar cells in bookshelf geometry. The liquid crystalline mixtures and individual compounds were filled into glass cells with indium tin oxide (ITO) transparent electrodes by means of capillarity action.

The miscibility of the compounds used for the mixtures was checked using the contact method of the cell preparation [29], which was useful also in some cases for the phase identification [30].

The X-ray diffraction studies (range of small diffraction angles in 2θ=1.3–5.0°) were done with modified DRON system equipped with Ge monochromator, working in reflection mode in order to obtain the layer thickness in smectic phases [31] ('small angles' method). Samples were prepared on a glass with one surface left free, which assured homeotropic alignment. Temperature was controlled within 0.1 K. The layer spacing has been calculated from the small diffraction angles.

In order to determine the intermolecular distance, non-oriented samples have been studied in a transmission geometry using conventional powder diffractometer, Philips PW 1350, CuKα radiation at 0.154 nm and Ni filter ('wide angles' method). The diffractograms of the investigated compounds were recorded in the range of large diffraction angles in 2θ=5–35°. The samples were deposited on the platinum measuring plate connected with the thermocouple Pt–10% RhPt. Sample temperature has been controlled by the temperature controller HTK2-HC (Paar) and the heating/cooling rate was 1 K min^{-1}.

The layer spacing (d) and the average intermolecular distance between the long axes of neighbouring parallel molecules (D) were performed using the Bragg law: $n\lambda=2d\sin\theta$. The parameters d and D were calculated from the position of the small angle and large angle diffraction peak, respectively [32, 33].

Results and discussion

Materials and mixture composition

Two new symmetrical star-shaped bent core compounds have been prepared according to the synthetic procedure depicted in Scheme 1.

The *bis*(ethyl-5-hydroxy)-isophthalate was reacted with the appropriate alkylbromide, than the ester protecting group was removed by hydrolysis. The 5-alkoxy-phthalic acid derivative (**1**) was converted to its acid chloride (**2**) and reacted with a phenol component (**3**) leading to the final product BI (n=10) and CI (n=4) (see Scheme). Chemical formulae with the respective estimated molecular lengths calculated by semiempirical MOPAC method are shown in Table 1.

Synthesis and mesomorphic properties of the compound AI were presented in [4]. This compound shows two enantiotropic mesophases: high temperature mesophase is the antiferroelectric smectic B2 phase; the lower temperature mesophase is the smectic B7 phase with in-plane ordering [34]. Below the B7

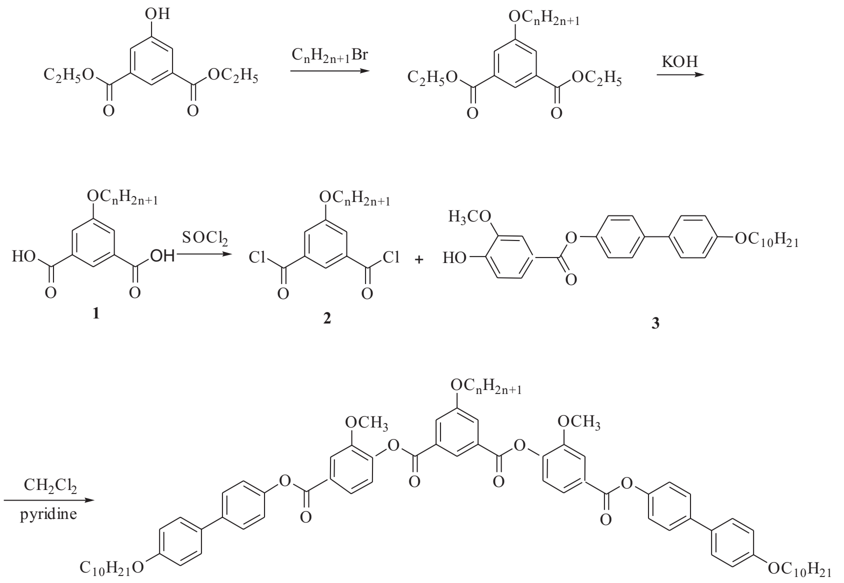

Scheme 1 Synthetic pathway for the preparation of new star-shaped bent core BI (*n*=10) and CI (*n*=4) compounds

phase, this compound possesses a low temperature monotropic crystal phase that can be clearly seen on DSC scan (Fig. 1). The peak at 106°C due to relatively large enthalpy corresponds to the phase transition to a crystal phase (denoted here as CrX phase) – the structure of the phase is not identified yet.

The chiral rod like compound AII possess a very broad enantiotropic paraelectric orthogonal smectic A (SmA*) phase. Synthesis and physical properties of this compound were described in [26]. The phase transition of the compounds AI and AII are included in Table 3.

Compounds BI and CI are new bent core compounds with seven phenyl rings presented in this paper. Their chemical structure is similar to compound AI with an alkyl chain of various lengths as a

Table 1 Chemical formulae of the compounds used for the binary mixtures, the length of molecules (L) and their parts [Å]

Code	Chemical formulae	$L^{a,b}$/Å
AI	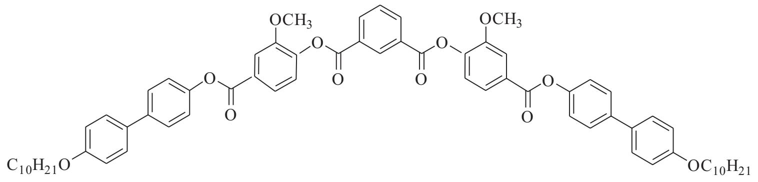	52 30^c
AII	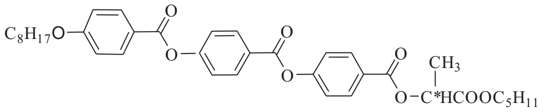	37
BI	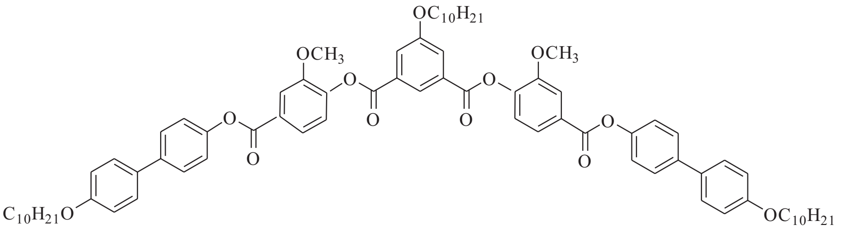	52 17^d
BII	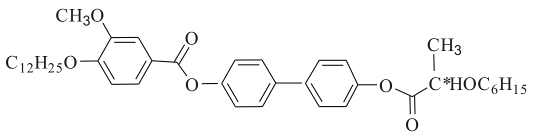	42

^{a}calculated for the most extended conformers; ^{b}error of calculations δ_L±0.5 Å; ^{c}wing length; ^{d}length of alkyl chain at the central ring

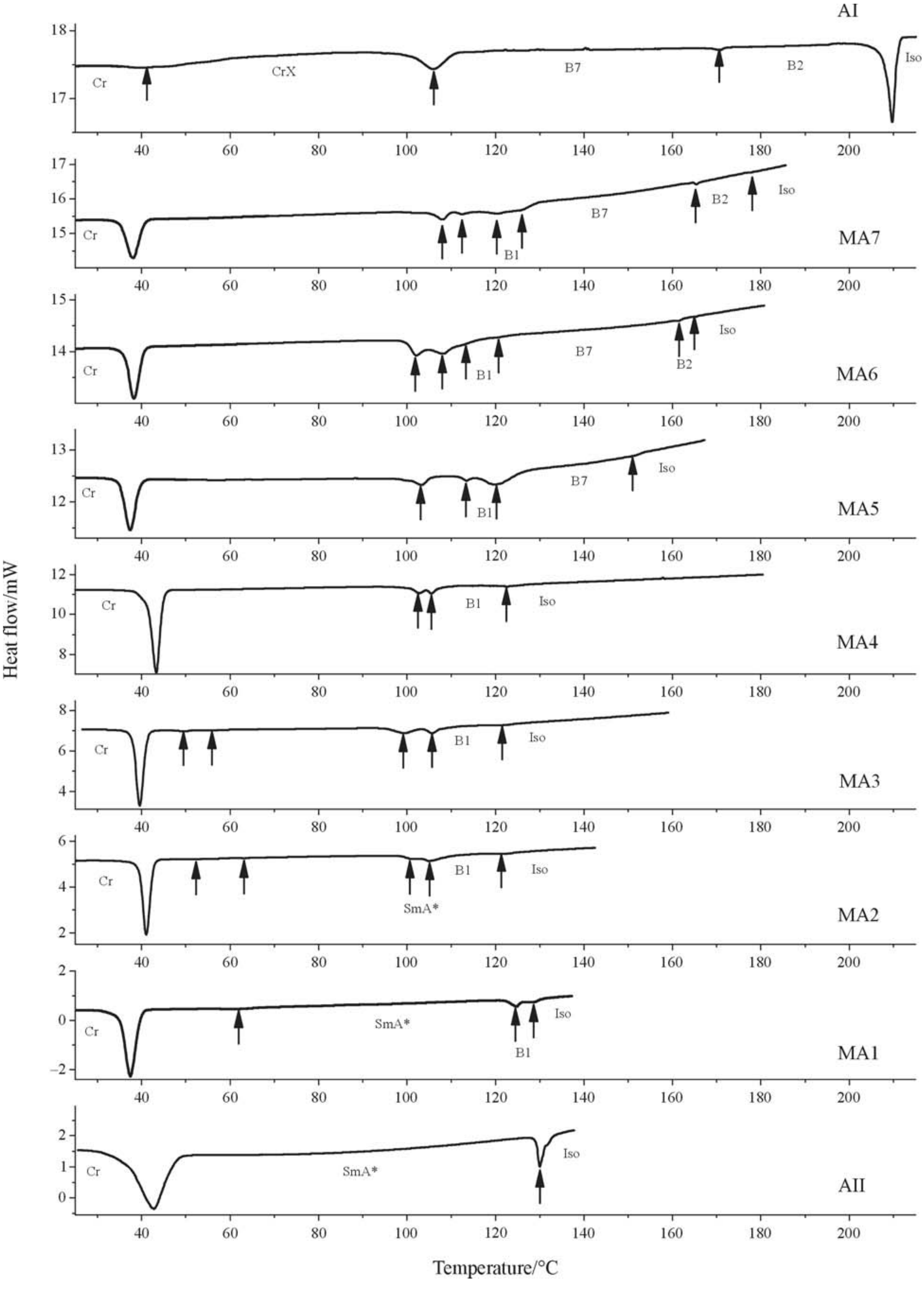

Fig. 1 DSC plots of MA-series obtained on cooling. Arrows indicate peaks corresponding to phase transitions

Table 2 Mixture composition of the MA and MB series

Code	mol. mass/ g mol^{-1}	AI	AII	BI	BII
		mol%			
AII	630	0	100	–	–
MA1	766	3	97	–	–
MA2	779	11	89	–	–
MA3	838	13	87	–	–
MA4	915	15	85	–	–
MA5	1014	37	63	–	–
MA6	1023	54	46	–	–
MA7	1032	67	33	–	–
MA8	1068	70	30	–	–
AI	1082	100	0	–	–
BII	685	–	–	0	100
MB1	857	–	–	10	90
MB2	1017	–	–	21	79
MB3	1123	–	–	40	60
MB4	1184	–	–	69	31
BI	1239	–	–	100	0

substituent on the central phenyl ring at the meta position to carboxyl group. These star-shaped banana compounds did not exhibit mesophases most probably due to the substituent connected to the central ring. Compound CI was studied by polarizing optical microscopy and DSC (melting point 137.3°C with enthalpy ΔH=+33.9 J g^{-1} and crystallization at 100.4°C with enthalpy ΔH=[–15.9 J g^{-1}]). This compound was not selected for mixture preparation.

Synthesis and mesomorphic properties of the chiral rod like compound BII were described in [27] and [28]. This compound possesses a rich variety of mesophases: the enantiotropic chiral nematic (N*), the enantiotropic paraelectric SmA*, the enantiotropic tilted ferroelectric smectic C* (SmC*) phases. A monotropic lower temperature non-tilted smectic phase appears (probably the SmB with hexatic ordering of the long molecular axis) before the crystallization.

Two series of mixtures composed of the bent core and rod like molecules have been prepared and studied, namely the system of AI and AII (denoted as MA-series) and system of BI and BII (denoted as MB-series). The composition of the mixtures in molar percent is summarised in Table 2.

Thermal and mesomorphic properties of MA mixtures

Mixtures composed from AI (bent shaped) and AII (rod like) compounds were prepared in order to lower the temperature range of the bent type compound possessing B2 and B7 phases. The rod like compound AII exhibits the enantiotropic SmA* mesophase within a broad temperature range (Table 3). Preliminary investigation for the phase diagrams was carried out by contact preparation method. In binary mixtures the original phase of the individual compounds could be preserved and in some cases their temperature range has been enlarged. In a few cases induction of a new mesophase was also observed (Table 3). It is supposed that compound AII can be accommodated in the banana host (AI) because the wing of banana is comparable in length with compound AII (Table 1). The phase transition temperatures and enthalpy changes of MA mixtures are summarized in Table 3.

On Fig. 2 the textures obtained by contact cell preparation of the bent core compound AI (left side) and rod like compound AII (right side) are presented. On Fig. 2a, the planar texture of the B2 phase done at 190°C is observed on the left side. The right side corresponds to the rod like compound AII being at the isotropic phase at this temperature. Microphotograph of texture presented on Fig. 2b taken at 130°C possesses wider area of the B7 phase (about 70% of B7 and about 30% of the isotropic phase). At 105°C, the crystallization of the LCX phase occurs as a front starting from the left-side (Fig. 2c). A narrow area of the SmA phase still remains due to a high concentration of the rod like compounds AII on the right side.

Textures obtained in the planar cell (6 μm) for the mixture MA5 are shown on Fig. 3a–c. The B7 phase is growing from the isotropic phase at about 150°C as it is shown on Fig. 3a with crossed polarizers and on Fig. 3b without polarizers. Filaments, spirals and ribbons characteristic to this phase can be clearly seen on the texture. On Fig. 3c taken at 117°C, the induced columnar B1 phase is presented.

For the mixture MA3 the characteristic texture of the induced B1 phase is shown on Fig. 4: (a) – iso-

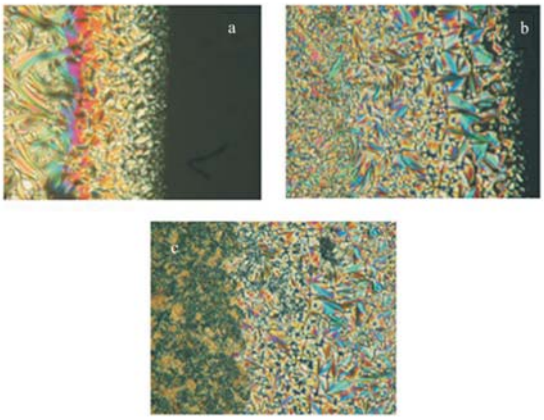

Fig. 2 Textures obtained by contact cell preparation with bent core compound AI (left side) and rod like compound AII (right side) under crossed polarizers: at a – 190°C; b – 130°C; crystallization occurs as a front at c – 105°C

Table 3 Rich polymorphism and sequence of phases of the liquid crystalline binary mixtures of MA-series: phase transition temperatures T_c [°C], transition enthalpies ΔH [J g^{-1}] (in square brackets) evaluated on cooling and melting points *m.p.* [°C]

code	*m.p.*		T_c		T_c		T_c		T_c		T_c		T_c		T_c		T_c		T_c	
AII	69.7 [+39.3]	Cr	41.8 [–38.1]									SmA*	130.0 [–5.4]							Iso
MA1	53.3 [+29.5]	Cr	37.3 [–29.1]					LCX	61.0 [–1.7]			SmA*	124.8 [–1.2]	B1	128.6 [–0.3]					Iso
MA2	53.4 [+26.0]	Cr	41.1 [–22.8]			LCX	52.8 [–0.2]	LCX	63.4 [–0.1]	LCX	100.9 [–0.4]	SmA*	104.9 [–1.7]	B1	122.3 [–1.2]					Iso
MA3	53.5 [+24.7]	Cr	39.6 [–25.0]	LCX	49.8 [–0.4]	LCX	55.8 [–0.2]	LCX	99.6 [–2.6]	LCX			105.7 [–1.9]	B1	121.7 [–1.4]					Iso
MA4	68.6 [+35.2]	Cr	43.3 [–32.1]					LCX	102.6 [–1.0]	LCX			105.5 [–1.1]	B1	122.9 [–2.0]					Iso
MA5	58.9 [+20.7]	Cr	37.4 [–15.4]					LCX	103.2 [–3.3]	LCX			113.5 [–0.5]	B1	120.8 [–5.6]	B7	150.8 [–4.3]			Iso
MA6	52.7 [+10.9]	Cr	38.3 [–11.5]			LCX	102.1 [–1.9]	LCX	108.3 [–2.1]	LCX			115.9 [–0.3]	B1	120.0 [–0.1]	B7	161.6 [–0.3]	B2	165.4 [–0.1]	Iso
MA7	60.6 [+12.8]	Cr	38.4 [–12.5]			LCX	108.1 [–1.7]	LCX	112.6 [–0.4]	LCX			120.3 [–0.5]	B1	126.1 [–0.9]	B7	165.5 [–0.2]	B2	178.3 [–0.1]	Iso
MA8	155.4 [+21.6]	Cr	99.7 [–7.8]						LCX	121.6 [–0.2]						B7	167.2 [–0.1]	B2	186.4 [–0.3]	Iso
AI	157.0 [+25.8]	Cr	45.1 [–10.1]	CrX	106.0 [–11.1]											B7	170.7 [–0.7]	B2	209.6 [–21.2]	Iso

Iso – isotropic phase; Cr – highly ordered crystal phase; CrX – crystal phase modification; LCX – undetermined liquid crystalline phase

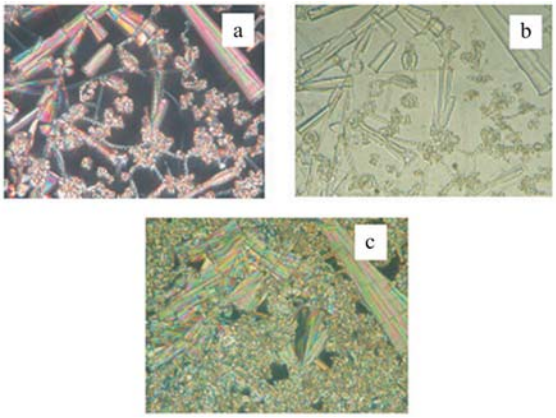

Fig. 3 Textures obtained in the planar cell (6 μm thick) for the mixture MA5: Iso-B7 phase transition at 150°C a – under crossed polarizers and b – without polarizers; c – B1 phase at 117°C

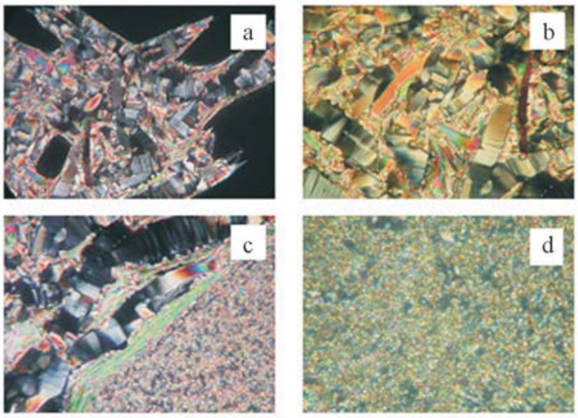

Fig. 4 Textures obtained in the planar cell (6 μm thick) for the mixture MA3 under crossed polarizers: Iso-B1 phase transition at a – 121°C; b – B1 phase at 115°C; c – B1-LCX phase transition at 105°C; d – LCX phase at 80°C

tropic-B1 phase transition and (b) – the mosaic texture of B1 phase at 115°C. The transition to the undetermined LCX phase occurs at 105°C (Fig. 4c). The grainy texture of the LCX phase taken at about 80°C is shown on Fig. 4d.

X-ray diffraction studies were carried out on the individual compounds and selected binary mixtures in order to measure the layer spacing and intermolecular distance in different phases. A diffuse scattering maximum in the wide angle region can be observed in B2 and B7 phases at indicated temperatures. Intermolecular average repeat distance (D) between the neighbouring molecules of compounds AI and AII and selected mixtures was determined by the ‘wide angles’ method, the results are summarised in Table 4. The shift of the maximum of the broad peak towards higher angle values, and hence the decrease of the intermolecular distance (Table 4), indicates the increase of the packing density with temperature decrease. That was observed for individual rod like and bent shaped compounds and their mixtures as well.

The layer spacing for the rod like and bent shaped compounds has been determined using ‘small angles’ method. The X-ray pattern exhibits a sharp peak at small angles which indicates a layered structure. The temperature dependence of the layer spacing and respective peak intensity is shown on Fig. 5 for AII and AI compounds. A slight increase of the layer spacing in the orthogonal SmA* phase (for about 1 Angstrom within temperature range about 45 K) is due to increase of the ordering with temperature decrease (Fig. 5a). For the AI (Fig. 5b), there is a slight decrease of the layer spacing with temperature decrease in the B2 phase, while d remains nearly constant within the B7 phase. The phase transition to the CrX (Fig. 5b) phase occurs at higher temperature (124°C) than it is indicated in Table 3 as the B7 phase below the melting point (157°C) has the monotropic character. For the rod like compound, the measured layer spacing in the orthogonal SmA* phase is slightly higher than the calculated molecular length, which indicates the low positional ordering. No remarkable difference can be found between the layer spacing of the bent shaped compound AI and its calculated molecular length (Table 1).

Since ‘small angles’ method used for the determination of the layer spacing, it needs a specific alignment of the samples. There were difficulties in obtaining such a homeotropic alignment in case of the mixtures. More detailed information on the structure of mesophases, an advanced structural synchrotron study is necessary and will be presented elsewhere.

Table 4 Intermolecular average repeat distance D [Å] determined from the reflection at large angle (12°<2θ<30°) for compounds AI, AII and their binary mixtures in detected mesophases at the indicated temperatures T [°C]

code	phase	T/°C	D/Å
AII	Iso	150	5.179
	SmA*	115	5.091
MA5	Iso	170	5.209
	B7	140	5.005
	B1	118	4.790
MA6	Iso	166	5.240
	B2	163	4.665
	B1	118	4.547
MA8	Iso	188	5.120
	B2	175	4.524
AI	Iso	226	5.533
	B2	190	5.399
	B7	155	5.334

D – for the intermolecular average repeat distance,
δ_D – error of measurements was about ±0.002 Å

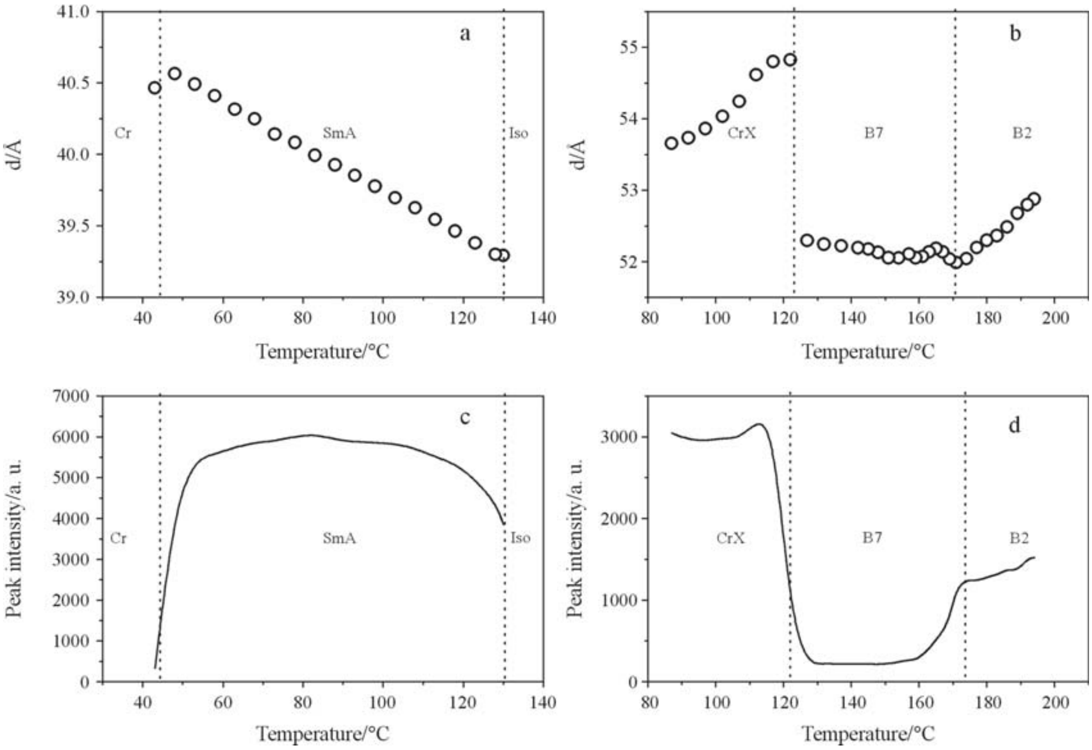

Fig. 5 Temperature dependences of the layer spacing for the a – AII and b – AI determined from the reflection by 'small angles' method within $1.3° < 2\theta < 4°$. The related temperature dependences of the c and d – peak intensity and for the AII and AI, respectively. Error of measurements δ_d was about ±0.2 Å

Thermal and mesomorphic properties of MB mixtures

Second type of the mixtures (MB series) has been studied in order to induce mesomorphic properties in mixtures of the non-liquid crystalline star-shaped bent core compound BI and the liquid crystalline chiral rod like material BII exhibiting a rich variety of mesophases. Mixtures MB1-MB4 were prepared and their percentage composition are presented in Table 2. Rich polymorphism and sequence of phases of the liquid crystalline binary mixtures of MB-series are presented in Table 5. Figure 6 depicts DSC plots measured on cooling of individual compounds BI and BII, as well as their indicated mixtures. The respective phase diagram obtained on cooling is shown on Fig. 7. The chiral nematic phase is very sensitive and disappears in the mixtures studied (Table 5, Fig. 7).

The paraelectric SmA* and the ferroelectric SmC* phases are still present even in the mixture MB3. The SmB phase appears in all four studied mixtures and is still present even with minor presence of the rod like compound BII. The eutectic behaviour is observable in the melting points – the lowest one at

Table 5 Rich polymorphism and sequence of phases of the liquid crystalline binary mixtures of MB-series: phase transition temperatures T_c [°C], transition enthalpies ΔH [J g^{-1}] (in square brackets) evaluated on cooling and melting points *m.p.* [°C]

Code	*m.p.*		T_c		T_c		T_c		T_c		T_c	
BII	67.7 [+28.8]	Cr	38.8 [–20.1]	SmB	56.8 [–2.3]	SmC*	79.6 [–0.6]	SmA*	85.2 [msc]	N*	88.0 [–4.6]	Iso
MB1	64.2 [+18.9]	Cr	27.1 [–12.5]	SmB	43.5 [–1.4]	SmC*	66.2 [–1.0]	SmA*	78.4 [–1.9]	Iso		
MB2	63.1 [+26.0]	Cr	20.5 [msc]	SmB	40.5 [–1.4]	SmC*	58.5 [–1.6]	SmA*	66.1 [–0.1]	Iso		
MB3	47.8 [+2.8]	Cr	41.3 [–2.2]	SmB	61.1 [msc]	SmC*	65.4 [–2.0]	Iso				
MB4	68.2 [+0.4]	Cr	65.8 [–1.2]	SmB	86.3 [–2.2]	Iso						
BI	90.2 [+6.1]	Cr	89.1 [–8.1]	Iso								

[msc] – determined by microscope only; Cr – highly ordered crystal phase

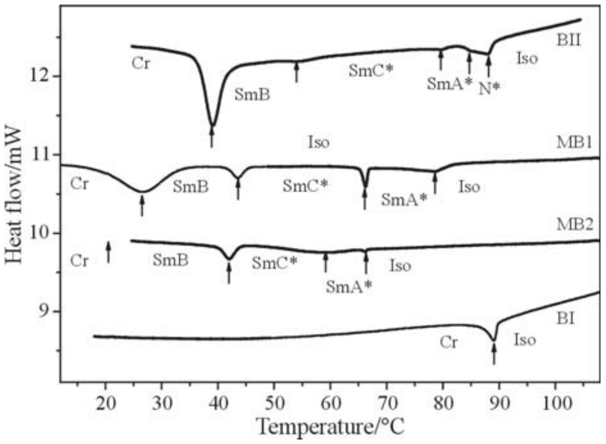

Fig. 6 DSC plots of BI, BII and indicated MB-mixtures obtained on cooling. Arrows indicate peaks corresponding to phase transitions

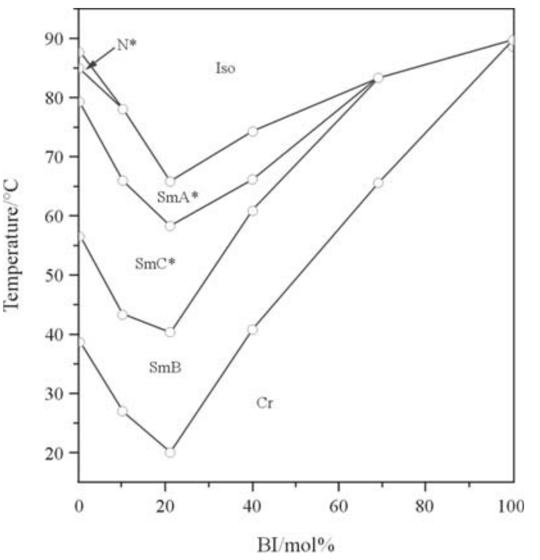

Fig. 7 Phase diagram obtained on cooling from the isotropic phase of the MB mixtures composed from BI and BII

47.8°C corresponds to the mixture MB3 with 40 mol% of the bent core molecules. The MB2 is proved to be the most supercoolable mixture possessing the lowest temperature of crystallization.

Conclusions

Two new star-shaped bent core compounds were synthesised and studied. Binary mixtures composed from bent core and chiral rod like and star-shaped bent core compounds are prepared. Their thermal, mesomorphic and structural properties are investigated in order to contribute to the understanding of the miscibility and structure-property relationship of these materials.

Mixtures of compounds AI and AII denoted as MA1-MA8 show a very complex behaviour. In mixtures where the bent core compound was present in higher concentration the B2 and B7 phases were preserved. On the opposite, the SmA* phase is preferential at high concentration of the rod like compound. The B2 phase appeared in mixtures MA6-MA8; the B7 phase was observed in mixtures MA5-MA8. The induction of the B1 phase is postulated (Fig. 4b) in almost every mixture studied. Several types of liquid crystalline phases (denoted generally as LCX) were detected by DSC in the most mixtures studied. The advanced structural characterization of these phases is planned by X-ray diffraction on oriented samples and will be presented elsewhere.

The compounds of the quite different architectures were mixed and studied. The individual star-shaped bent core compound BI without mesomorphic behaviour, prepared especially for these studies, was mixed with chiral rod like compound BII exhibiting a rich polymorphism. As a result, the ‘calamitic phases’, i.e. phases formed by the rod like molecules, were dominating in all the mixtures (MB1–MB4) investigated. The chiral nematic phase of the compound BII was suppressed in all the mixtures but the paraelectric SmA* and ferroelectric SmC* phases remain in MB1 and MB2. The hexatic orthogonal SmB phase of compound BII is detected in all mixtures studied.

It can be concluded on the basis of these investigations, that in mixtures MA, the ‘banana phases’ are dominating; on the contrary MB mixtures exhibit rather the mesophases characteristic to the rod like compounds.

Acknowledgements

This work was supported by bilateral agreement of the Hungarian Academy of Sciences and Academy of Sciences of the Czech Republic, Project ESF COST D35 WG 13-05, Grants No. 202/05/0431 from the Czech Science Foundation, No. IAA100100710 from the Grant Agency of the Academy of Sciences of the Czech Republic, No. 141020 from the Ministry of Science and Environmental of Republic of Serbia and the Hungarian Research Grant OTKA TO37336 and OTKA K61075. Authors are grateful to Dr. P. Vanek for technical support with DSC measurements.

References

1 T. Sekine, T. Niori, M. Sone, J. Watanabe, S.-W. Choi, Z. Takanishi and H. Takezoe, Jpn. J. Appl. Phys., 36 (1997) 6455.
2 J. Thaisayukta, H. Takezoe and J. Watanabe, Jpn. J. Appl. Phys., 40 (2001) 3277.
3 H. Takezoe and Y. Takanishi, Jpn. J. Appl. Phys., 45 (2006) 597.
4 M. Kašpar, V. Hamplová, V. Novotná, M. Glogarová and P. Vanek, J. Mater. Chem., 12 (2002) 2221.

5 D. M. Walba, L. Eshdat, E. Körblova and R. K. Shoemaker, Cryst. Growth Des., 5 (2005) 2091.
6 A. Eremin, I. Wirth, S. Diele, G. Pelzl, H. Schmalfuss, H. Kresse, H. Nádasi, K. Fodor-Csorba, E. Gács-Baitz and W. Weissflog, Liq. Cryst., 29 (2002) 775.
7 K. Fodor-Csorba, A. Vajda, A. Jákli, C. Slugovc, G. Trimmel, D. Demus, E. Gács-Baitz, S. Holly and G. Galli, J. Mater. Chem., 14 (2004) 2499.
8 D. R. Link, G. Natale, R. Shao, J. E. Maclennan, N. A. Clark, E. Körblova and D. Walba, Science, 278 (1997) 1924.
9 N. Niwano, M. Nakata, J. Thaisayukta, D. R. Link, J. Takezoe and J Watanabe, J. Phys. Chem. B, 108 (2004) 14889.
10 J. Watanabe, T. Niori, T. Sekine and H. Takezoe, Jpn. J. Appl. Phys., 37 (2001) L139.
11 Y. Takanishi, G. J. Shin, J. C. Jung, S.-W.Choi, K. Ishikawa, J. Watanabe, H. Takezoe and P. Toledano, J. Mater. Chem., 15 (2005) 4020.
12 E. Gorecka, M. Nakata, J. Mieczkowski, Y. Takanishi, K. Ishikawa, J. Watanabe, H. Takezoe, S. H. Eichhorn and T. M. Swager, Phys. Rev. Lett., 85 (2000) 2526.
13 E. Gorecka, M. Čepič, J. Mieczkowski, M. Nakata, H. Takezoe and B. Žekš, Phys. Rev. E, 67 (2003) 061704.
14 K. D'have, A. Dahlgren, P. Rudquist, J. P. F. Lagerwall, G. Andersson, M. Matuszczcyk, S. T. Lagerwall, R. Dabrowski and W. Drzewinski, Appl. Phys. Lett., 76 (2000) 3528.
15 F. Goc, Ch. Selbmann, S. Rauch, H. Geppke and R. Dabrowski, Mol. Cryst. Liq. Cryst., 439 (2005) 147.
16 W. Weissflog, L. Kovalenko, I. Wirth, S. Diele, G. Pelzl, H. Schmalfuss and H. Kresse, Liq. Cryst., 27 (2000) 677.
17 L. Kovalenko, W. Weissflog, S. Grande, S. Diele, G. Pelzl and I. Wirth, Liq. Cryst., 27 (2000) 683.
18 I. Wirth, S. Diele, A. Eremin, G. Pelzl, S. Grande, L. Kovalenko, N. Pancenko and W. Weissflog, J. Mater. Chem., 11 (2001) 1642.
19 W. Weissflog, H. Nádasi, U. Dunemann, G. Pelzl, S. Diele, A. Eremin and H. Kresse, J. Mater. Chem., 11 (2001) 2748.
20 M.W. Schröder, S. Diele, G. Pelzl, N. Pancenko and W. Weissflog, Liq. Cryst., 29 (2002) 1039.
21 J. Thisayukta, H. Niwano, H. Takezoe and J. Watanabe, J. Mater. Chem., 11 (2001) 2717.
22 R. Pratibha, N. V. Madhusudana and B.K. Sadashiva, Science, 288 (2000) 2184.
23 N. Sen, Curr. Sci., 79 (2000) 1417.
24 R. Pratibha, N. V. Madhusudana and B. K. Sadashiva, Pramana, 61 (2003) 405.
25 R. Pratibha, N. V. Madhusudana and B. K. Sadashiva, Phys. Rev. E, 71 (2005) 011701.
26 M. Kašpar, V. Hamplová, S. Pakhomov, A. M. Bubnov, F. Guittard, H. Sverenyák, I. Stibor, P. Vanek and M. Glogarová, Liq. Cryst., 24 (1998) 599.
27 M. Kašpar, H. Sverenyák, V. Hamplová, M. Glogarová, S. Pakhomov, P. Vanek and B. Trunda, Liq. Cryst., 19 (1997) 775.
28 M. Kašpar, V. Hamplová, S. Pakhomov, I. Stibor, H. Sverenyák, A. M. Bubnov, M. Glogarová and P. Vanek, Liq. Cryst., 22 (1997) 557.
29 H. Sackmann and D. Demus, Mol. Cryst. Liq. Cryst., 21 (1973) 239.
30 D. Demus, Chemical Compositions and Display Performance. Nonemissive Electrooptic Displays, A. R. Kmetz and F. K. von Willisen, Eds, Plenum Press, New York 1976, p. 92.
31 V. Hamplová, A. Bubnov, M. Kašpar, V. Novotná, D. Pociecha and M. Glogarová, Liq. Cryst., 30 (2003) 627.
32 D. Ž. Obadović, A. Vajda, T. Tóth-Katona and R. Marinković-Nedučin, Mol. Cryst. Liq. Cryst., 265 (1995) 135.
33 M. Garić, D. Ž. Obadović, A. Bubnov, V. Hamplová, M. Kašpar and M. Glogarová, Mol. Cryst. Liq. Cryst., 412 (2004) 587.
34 V. Novotna, M. Kašpar, V. Hamplova, M. Glogarová, K. Knižek, S. Diele, G. Pelzl, Ch. Jones, D. Coleman and N. A. Clark, Liq. Cryst., 32 (2005) 967.

Received: August 4, 2006
Accepted: November 21, 2006
OnlineFirst: April 29, 2007

DOI: 10.1007/s10973-006-7913-7